Spatially Resolved CPTu Monitoring of Enzyme-Induced Cementation Fronts

Clara Weiß[1], Jan L. Graf[2]

[1] Department of Architecture, TUM School of Engineering and Design, Technical University of Munich, Munich, Bavaria, Germany
[2] Department of Architecture, TUM School of Engineering and Design, Technical University of Munich, Munich, Bavaria, Germany

Abstract

The demand for sustainable and environmentally benign ground improvement techniques has driven significant advancements in biogeochemical soil stabilization methods. Enzyme-Induced Carbonate Precipitation has emerged as a particularly promising alternative to conventional Portland cement-based grouting, offering a lower carbon footprint and reduced ecological disturbance. However, the spatial variability of the precipitated calcium carbonate and the complex dynamics of the moving cementation front pose substantial challenges for quality assurance and field verification. This paper presents a comprehensive investigation into the application of Piezo-cone penetration testing for the spatially resolved monitoring of Enzyme-Induced Carbonate Precipitation cementation fronts in granular soils. Through large-scale calibration chamber experiments, the mechanical response of the biocemented soil was continuously profiled, allowing for the precise delineation of treated boundaries and transition zones. The research establishes robust correlations between localized penetration resistance, pore water pressure dissipation, and the spatially distributed calcium carbonate content. The findings demonstrate that high-resolution continuous profiling can effectively capture the heterogeneous architecture of the cementation front, providing crucial insights into injection efficiency and biocement distribution. This methodology offers a scalable and minimally invasive framework for real-time monitoring and verification of biogeochemical ground improvement processes in field applications.

Keywords: Enzyme-Induced Carbonate Precipitation; Cone Penetration Testing; Ground Improvement; Spatial Monitoring

1. Introduction

1.1 The Imperative for Sustainable Soil Improvement

The global construction industry is increasingly recognizing the urgent need to transition toward sustainable engineering practices. Traditional soil improvement techniques, predominantly those relying on Portland cement for deep soil mixing, jet grouting, and permeation grouting, are associated with immense carbon dioxide emissions and significant environmental degradation. The production of ordinary Portland cement is one of the largest anthropogenic sources of greenhouse gases, contributing to a substantial percentage of global carbon emissions. Furthermore, the high alkalinity of cementitious grouts can permanently alter the local groundwater chemistry, rendering it hazardous and disrupting subterranean ecosystems. In response to these pressing environmental concerns, geotechnical engineers and researchers have been actively exploring alternative ground modification techniques that align with the principles of sustainable development and green engineering. The shift away from energy-intensive chemical binders has catalyzed a multidisciplinary effort to harness natural biochemical processes for engineering applications [1]. This paradigm shift is not merely a theoretical exercise but a practical necessity driven by increasingly stringent environmental regulations and a growing societal demand for low-impact infrastructure development. The exploration of biomediated and bioinspired geotechnics represents a frontier in civil engineering, where biological mechanisms are adapted to enhance the mechanical and hydraulic properties of geomaterials without the adverse environmental footprint associated with conventional methods [2].

1.2 Advancements in Biogeochemical Ground Modification

Among the various sustainable ground improvement technologies under investigation, biogeochemical techniques have garnered the most attention due to their efficacy and adaptability. Enzyme-Induced Carbonate Precipitation is a premier example of this innovation. Unlike Microbially Induced Carbonate Precipitation, which relies on the in-situ cultivation and stimulation of living bacteria to produce the urease enzyme, Enzyme-Induced Carbonate Precipitation utilizes free urease enzymes extracted directly from agricultural sources such as jack beans. This distinction is critical for field applications, as it eliminates the complexities associated with biological cultivation, oxygen supply, and bacterial transport through porous media [3]. The introduction of a biochemical solution containing the free urease enzyme, urea, and a calcium source into the soil matrix triggers a series of biochemical reactions that culminate in the precipitation of calcium carbonate crystals at the particle contact points. These crystals serve as biological bridges, effectively cementing the loose sand grains together, thereby increasing the shear strength and stiffness of the soil while concomitantly reducing its hydraulic conductivity [4]. The flexibility of the enzymatic approach allows for greater control over the reaction kinetics and the final spatial distribution of the cementation, making it a highly attractive solution for a wide range of geotechnical challenges, including liquefaction mitigation, slope stabilization, and fugitive dust control. However, the successful field implementation of this technology requires a profound understanding of how the biochemical solutions migrate and react within heterogeneous geological formations [5].

1.3 The Role of In-Situ Monitoring

Despite the significant biochemical advancements in precipitation technologies, the transition from controlled laboratory experiments to full-scale field deployment is heavily hindered by the lack of reliable quality control and quality assurance mechanisms. In standard laboratory settings, the efficacy of the cementation process is typically evaluated through destructive testing methods, such as unconfined compressive strength tests or direct shear tests, performed on uniformly treated small-scale samples. While these tests provide fundamental mechanical parameters, they are entirely inadequate for assessing the spatial distribution of cementation in large-scale applications. When biochemical solutions are injected into the ground, they do not propagate uniformly; instead, they follow paths of least resistance, leading to preferential flow, localized cementation, and the formation of complex, highly variable treated zones [6]. The boundary between the heavily cemented soil and the untreated virgin soil is known as the cementation front. Accurately mapping this front and understanding the spatial gradient of cementation within the treated volume is critical for validating the engineering design and ensuring the safety of the overlying structures [7]. Traditional site investigation tools often lack the spatial resolution required to detect the subtle gradients associated with biochemical cementation, necessitating the development of specialized monitoring strategies. Piezo-cone penetration testing has emerged as a highly promising candidate for this task, offering continuous, high-resolution measurements of mechanical and hydraulic properties as the probe is advanced into the subsurface [8].

1.4 Research Objectives and Scope

The primary objective of this comprehensive study is to investigate the capabilities and limitations of spatially resolved Piezo-cone penetration testing for monitoring Enzyme-Induced Carbonate Precipitation cementation fronts in granular soils. Specifically, this research aims to characterize the mechanical signature of the moving cementation boundary by analyzing continuous profiles of tip resistance, sleeve friction, and penetration-induced pore water pressure. By conducting large-scale calibration chamber experiments under carefully controlled stress conditions, the study seeks to establish robust empirical and semi-empirical correlations between the localized penetration metrics and the actual spatially distributed calcium carbonate content. A further objective is to evaluate the influence of different injection strategies and biochemical solution concentrations on the morphological development of the cementation front, and to determine how these variations manifest in the penetration testing data. The scope of this research is intentionally broad, encompassing soil preparation, complex biochemical formulation, advanced instrumentation, rigorous testing protocols, and multifaceted data analysis. Through this extensive investigation, the paper endeavors to provide a foundational framework that will enable geotechnical practitioners to utilize continuous profiling technologies for the real-time, in-situ verification of sustainable biogeochemical ground improvement projects.

2. Background and Literature Review

2.1 Biochemical Mechanisms of Enzyme-Induced Carbonate Precipitation

The fundamental mechanism underlying Enzyme-Induced Carbonate Precipitation is a two-step biochemical reaction that leverages the catalytic power of the urease enzyme. The first step involves the hydrolysis of urea. When the urease enzyme is introduced into an aqueous solution containing urea, it acts as a catalyst to break down the urea molecules into ammonia and carbonic acid. This initial reaction is highly dependent on the activity level of the enzyme, the temperature of the environment, and the ambient hydrogen ion concentration. As the hydrolysis proceeds, the ammonia rapidly equilibrates with water to form ammonium and hydroxide ions [9]. The generation of hydroxide ions leads to a significant increase in the alkalinity of the pore fluid, which is a critical prerequisite for the subsequent precipitation phase. Concurrently, the carbonic acid dissociates into bicarbonate and carbonate ions, a process that is also heavily influenced by the rising alkalinity. The second step is the actual precipitation of calcium carbonate. When a soluble calcium source, typically calcium chloride, is present in the pore fluid, the calcium ions react with the newly formed carbonate ions to precipitate solid calcium carbonate. The precipitation preferentially occurs at the contact points between the soil grains, as these regions provide favorable nucleation sites due to surface tension and menisci effects. The continuous growth of these crystals eventually forms solid bridges that interlock the granular matrix, transforming a loose, cohesionless soil into a synthetic sandstone [10].

2.2 Spatial Variability and the Cementation Front Phenomenon

One of the most complex phenomena encountered in biogeochemical ground improvement is the development and migration of the cementation front. When the biological reagents are injected into the soil from a central point, the concentration of the reactants is highest near the injection source. Consequently, the rate of calcium carbonate precipitation is maximum in the immediate vicinity of the injection well, leading to rapid and heavy cementation. As the fluid permeates radially outward, the concentration of the active ingredients gradually depletes due to continuous consumption by the precipitation reactions [11]. Furthermore, the precipitation of calcium carbonate near the injection point inevitably reduces the local porosity and intrinsic permeability of the soil, which in turn alters the subsequent flow paths of the injected fluid. This dynamic interplay between fluid flow, biochemical reaction kinetics, and evolving porous media properties results in a highly heterogeneous distribution of cementation. The cementation front is not a sharp, well-defined boundary; rather, it is a diffuse transitional zone characterized by a spatial gradient of calcium carbonate content, decreasing from the heavy cementation near the source to the zero cementation of the native soil [12]. Understanding the morphology, extent, and sharpness of this front is essential for determining the required spacing of injection wells and the total volume of reagents needed to achieve contiguous treatment.

2.3 Traditional Monitoring Techniques and Their Limitations

Historically, the evaluation of ground improvement techniques has relied heavily on conventional geotechnical investigation methods. Destructive sampling, such as coring, remains the gold standard for obtaining undisturbed samples for laboratory testing. However, retrieving high-quality cores from lightly to moderately cemented sandy soils is notoriously difficult, as the mechanical disturbance induced by the drilling process often fractures the biological cementation bonds, rendering the samples unrepresentative of the in-situ conditions. Furthermore, coring is a discrete point-sampling technique that provides no continuous information about the spatial variability between the boreholes [13]. Non-destructive geophysical methods, including electrical resistivity tomography and seismic cross-hole testing, have been widely investigated as alternatives. Electrical resistivity tomography capitalizes on the change in pore fluid conductivity and the displacement of conductive pore water by insulating calcium carbonate crystals to map the treated zone. While electrical methods provide valuable volumetric images, their spatial resolution decreases significantly with depth, and the inversion algorithms are susceptible to non-uniqueness problems, making it difficult to precisely delineate the boundaries of the cementation front [14]. Seismic methods, which measure the velocity of shear and compressional waves, offer excellent correlations with the small-strain stiffness of the treated soil. However, these techniques require complex source and receiver arrays, and the data interpretation can be heavily complicated by environmental noise and the specific site stratigraphy [15].

2.4 Principles of Piezo-Cone Penetration Testing in Cemented Geomaterials

Given the limitations of core sampling and geophysics, Piezo-cone penetration testing represents an optimal balance between high spatial resolution, mechanical relevance, and operational efficiency. The standard equipment consists of a cylindrical probe with a conical tip, which is pushed continuously into the ground at a constant rate. The instrument is equipped with load cells to measure the tip resistance and the sleeve friction, as well as a piezoelectric transducer to measure the dynamic pore water pressure generated during penetration. In uncemented granular soils, the tip resistance is primarily governed by the relative density, effective confining stress, and the internal friction angle of the material [16]. However, the introduction of biochemical cementation fundamentally alters the penetration mechanics. The calcium carbonate bonds impart a synthetic cohesion and stiffness to the soil, significantly increasing the force required to advance the cone. The tip resistance becomes a combined measure of the native soil state and the degree of biogeochemical cementation. Moreover, the failure mechanism ahead of the advancing cone shifts from a purely plastic cavity expansion mode in loose sands to a brittle, fracture-dominated mode in heavily cemented soils. The pore pressure response also provides critical diagnostic information. While loose, untreated sands typically exhibit contractive behavior and positive pore pressure generation during penetration, biocemented sands often demonstrate highly dilative behavior due to the disruption of the rigid, interlocked particle structure, resulting in characteristic negative pore pressure transients [17].

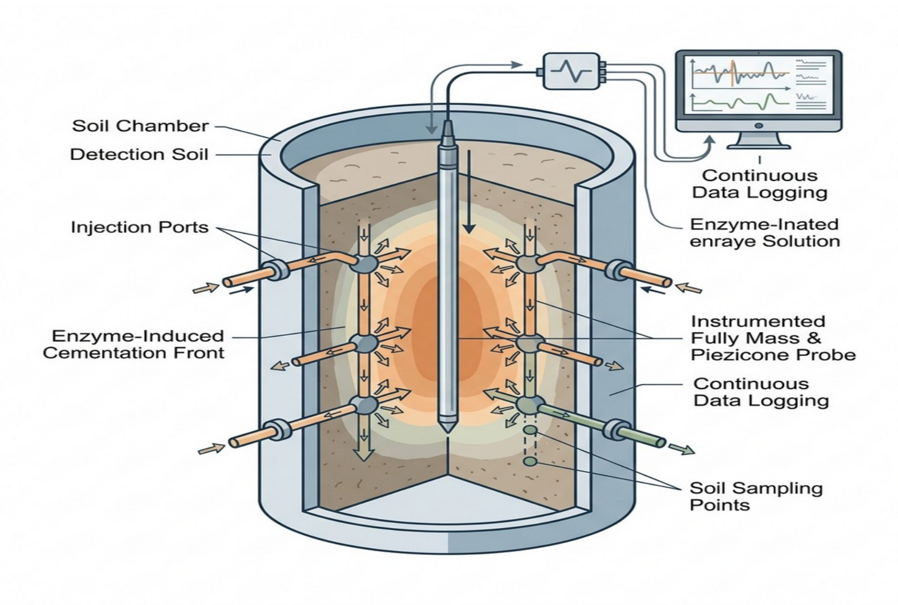

Figure 1: Comprehensive Schematic of the Large

3. Experimental Methodology and Setup

3.1 Geomaterial Characterization and Preparation

The experimental program was conducted using a standardized, commercially available silica sand, selected for its highly uniform grain size distribution and mineralogical purity. The material consisted of entirely quartz grains, ensuring that any subsequent biochemical reactions were strictly due to the introduced reagents and not influenced by native reactive minerals such as natural carbonates or expansive clays. The particle size distribution was carefully evaluated using mechanical sieve analysis, revealing a mean effective grain size that classified the material as poorly graded fine to medium sand according to the Unified Soil Classification System. The choice of a highly uniform sand was deliberate, as it minimizes the inherent natural spatial variability and allows for a more isolated study of the precipitation-induced heterogeneity [18]. To prepare the soil for the large-scale testing, the sand was thoroughly washed, oven-dried, and subsequently deposited into the testing vessel using a controlled dry pluviation technique. The pluviation process involved raining the sand through a series of diffusing meshes from a constant drop height to ensure a uniform initial relative density throughout the entire sample volume. The flow rate of the sand was continuously monitored and adjusted to maintain the target void ratio, which was selected to represent a naturally loose, liquefaction-susceptible deposit.

Table 1: Geotechnical and Physical Properties of the Base Silica Sand Material

Parameter Description	Measurement Value	Testing Standard Specification
Specific Gravity of Soil Solids	2.65	Standard Pycnometer Method
Minimum Achievable Void Ratio	0.52	Vibratory Compaction Protocol
Maximum Achievable Void Ratio	0.81	Loose Pouring Methodology
Mean Effective Particle Diameter	0.35 millimeters	Mechanical Sieve Analysis
Coefficient of Grain Uniformity	1.85	Particle Size Distribution

3.2 Biochemical Solution Formulation and Injection Strategy

The biochemical treatment process utilized a highly optimized, dual-phase injection protocol designed to maximize the spatial uniformity of the precipitation while preventing rapid, localized clogging near the injection source. The first phase involved the saturation of the soil matrix with a conditioning solution containing solely the free urease enzyme. The enzyme was extracted in the laboratory from jack bean meal using a low-temperature aqueous extraction process and subsequently purified using centrifugation and microfiltration. The specific activity of the urease solution was quantified using an electrical conductivity assay prior to every injection to ensure consistent catalytic potential across all experimental trials [19]. Following the enzyme conditioning phase, a second solution comprising the substrate and the structural components was introduced. This cementation fluid contained equimolar concentrations of analytical-grade urea and calcium chloride dihydrate. The injection system consisted of a central, multi-screened high-density polyethylene well positioned vertically within the soil mass. The fluids were delivered using a precision-controlled, non-pulsating peristaltic pump at a specifically engineered constant flow rate. The choice of a relatively low injection rate was intended to allow sufficient residence time for the biochemical reactions to occur within the pore space while enabling the fluid to permeate deeply into the granular matrix before the onset of significant permeability reduction.

3.3 Calibration Chamber Design and Instrumentation

To simulate realistic in-situ stress conditions and overcome the boundary effect limitations inherent in small bench-top experiments, a large-scale, flexible-wall calibration chamber was custom-engineered for this research. The chamber consisted of a thick-walled cylindrical steel outer shell and an inner flexible elastomeric membrane, creating an annular space that could be pressurized with water to apply a controlled radial confining stress to the soil sample. The top and bottom platens were fabricated from solid aluminum alloys and equipped with independent hydraulic systems to apply vertical boundary stresses, thereby allowing for the simulation of specific anisotropic consolidation states representative of varied burial depths [20]. The internal dimensions of the sample space were substantially larger than the standard zone of influence of the penetration probe, ensuring that the lateral boundaries did not artificially inflate the measured resistance parameters. The chamber was extensively instrumented with a three-dimensional array of miniaturized fluid pressure transducers and electrical conductivity sensors embedded directly within the soil mass during the pluviation process. These embedded sensors provided continuous, real-time, non-destructive tracking of the spatial progression of the reactive fluid front and the corresponding changes in pore water pressure during the injection phases.

3.4 Piezo-Cone Penetration Testing Execution Protocol

Upon the completion of the biochemical treatment and a subsequent curing period designed to allow for the complete consumption of the injected reagents, the continuous spatial monitoring phase was initiated. A miniature, laboratory-scale version of the standard Piezo-cone penetration probe was utilized to profile the treated volume. The miniaturized probe maintained the standard geometrical proportions, featuring a sixty-degree conical apex and a standardized ratio of friction sleeve area to projected tip area. The probe was advanced vertically into the treated soil at a strictly controlled standard penetration rate using a high-capacity, displacement-controlled electro-mechanical actuator mounted on a rigid reaction frame above the calibration chamber [21]. The data acquisition system recorded the outputs from the tip load cell, the sleeve load cell, and the pore pressure transducer at an exceptionally high sampling frequency, ensuring a spatial data resolution of less than one millimeter of vertical travel. To map the three-dimensional architecture of the cementation front, multiple penetration soundings were conducted within the same sample volume. The primary sounding was located immediately adjacent to the central injection well to capture the zone of maximum cementation, while subsequent soundings were performed at incrementally increasing radial distances from the source to profile the transition zone and locate the absolute outer boundary of the biochemical influence.

4. Spatial Resolution and Data Analysis Framework

4.1 Normalization of Penetration Parameters

The raw data acquired from the penetration testing requires sophisticated processing and normalization before meaningful correlations can be established regarding the spatial distribution of the biological cementation. As the cone probe advances deeper into the sample, the increasing overburden stress inherently causes a corresponding increase in the measured tip resistance, entirely independent of any cementation effects. To isolate the mechanical enhancement provided exclusively by the biochemical precipitation, the raw tip resistance must be normalized with respect to the initial effective vertical stress. This normalization is achieved by applying a stress-exponent methodology commonly utilized in traditional geotechnical engineering, which adjusts the measured parameters to an equivalent reference atmospheric pressure [22]. Furthermore, the penetration-induced pore water pressure is a highly dynamic variable that is heavily influenced by the degree of local cementation and the resulting dilative characteristics of the soil structure. To effectively utilize this parameter, a normalized pore pressure parameter is calculated by taking the difference between the measured dynamic pore pressure and the hydrostatic equilibrium pressure, and dividing this differential by the effective vertical stress. The simultaneous analysis of the normalized tip resistance and the normalized pore pressure parameter provides a comprehensive multiparameter framework for characterizing the highly variable mechanical behavior of the treated geomaterial.

4.2 Delineation of the Cementation Front

The identification and spatial mapping of the cementation front heavily relies on mathematical analysis of the gradients observed in the normalized penetration data. In the heavily cemented zone near the injection source, the normalized tip resistance exhibits massive, order-of-magnitude increases compared to the baseline values of the native, untreated sand. However, as the spatial boundary is approached, the penetration parameters do not drop to baseline values instantly; instead, they display a distinct, exponential decay curve indicative of the transition zone. The true boundary of the cementation front is defined mathematically as the spatial coordinate where the spatial derivative of the normalized tip resistance approaches zero, signifying that the resistance has returned to the stable baseline of the native soil [23]. To account for the natural signal noise inherent in mechanical testing, advanced signal processing techniques, specifically moving average filters and localized polynomial regression algorithms, are applied to the raw data sets to smooth the profiles before calculating the spatial derivatives. By analyzing multiple sounding locations at varying radial distances, a contour map of the spatial derivatives can be generated, effectively visualizing the three-dimensional morphology of the reaction front and highlighting areas of preferential flow or uneven treatment.

4.3 Correlation Models Between Mechanical and Biochemical Metrics

The ultimate goal of the data analysis framework is to translate the mechanical continuous profiling data into quantitative estimations of the actual biochemical output, specifically the spatial distribution of the precipitated calcium carbonate mass. Following the completion of all penetration soundings, the large-scale sample is systematically exhumed, and small, discrete samples are collected precisely from the locations corresponding to the path of the penetration probe. These physical samples undergo acid washing procedures to gravimetrically determine the exact calcium carbonate content by mass. A rigorous statistical analysis is then performed to correlate the localized physical mass data with the corresponding continuous mechanical data points. The analysis reveals a robust, highly non-linear relationship between the normalized tip resistance and the calcium carbonate content. The mathematical model capturing this relationship requires specific calibration parameters that account for the initial relative density of the soil and the baseline angularity of the particles.

Table 2: Empirical Framework for Interpreting Spatial Penetration Metrics in Cemented Sands

Cementation Degree Classification	Normalized Tip Resistance Range	Estimated Calcium Carbonate Content
Negligible to Zero Treatment	Less than fifty units	Below zero point five percent
Light to Moderate Transition Zone	Fifty to one hundred fifty units	Zero point five to two percent
Moderate to Heavy Treatment Zone	One hundred fifty to three hundred units	Two to four percent
Extremely Heavy Source Zone	Greater than three hundred units	Above four percent

5. Results and Discussion

5.1 Evolution of Penetration Resistance Profiles

The experimental results definitively demonstrate that continuous spatial profiling provides a highly sensitive and accurate reflection of the biogeochemical treatment efficacy. The penetration soundings conducted in close proximity to the central injection source displayed dramatic, erratic spikes in the normalized tip resistance, often reaching values that represent a five-fold to ten-fold increase over the untreated baseline parameters. This extreme resistance is a direct manifestation of the dense calcium carbonate crystalline networks that completely encase the sand grains and bridge the pore spaces in the primary reaction zone. Interestingly, the vertical profiles within this heavily treated zone rarely exhibited uniform resistance with depth. Instead, distinct layers of heightened cementation were routinely identified, particularly near the injection ports and at the lower boundaries of the sample where gravitational forces caused slight pooling of the reactive, dense calcium chloride solutions. The sleeve friction measurements also exhibited significant increases, although the magnitude of the increase was generally less pronounced than that of the tip resistance. The friction ratio, which is the mathematical quotient of the sleeve friction divided by the tip resistance, consistently decreased in the heavily cemented zones. This reduction is attributed to the fact that while the biocementation massively increases the necessary tip bearing force, the smooth, crystalline nature of the calcite precipitation can occasionally reduce the localized sliding friction along the side of the steel probe [24].

5.2 Mapping the Three-Dimensional Cementation Front

The strategic execution of multiple radial soundings facilitated the precise three-dimensional mapping of the transition zones and the terminal boundaries of the biochemical influence. As the testing locations moved progressively further from the injection source, the magnitude of the penetration resistance decreased in a highly predictable, non-linear fashion. At intermediate radial distances, the mechanical profiles became smoother, lacking the extreme brittle fracture spikes seen in the core zone, which indicates a shift from massive crystalline bridging to a more delicate, patchy cementation pattern that merely coats the particles without completely filling the void spaces. The exact location of the cementation front was clearly identifiable in the mechanical data as the critical point where the tip resistance curve asymptotically merged with the pre-established baseline parameters of the loose native sand. The mapping process revealed that the cementation front did not propagate as a perfect cylinder or sphere. Due to subtle, microscopic heterogeneities in the initial soil placement and localized variations in intrinsic permeability, the reaction fluids often created preferential fingering flow paths. The continuous penetration testing was exceptionally capable of detecting these anomalies, identifying thin, highly cemented horizontal lenses extending far beyond the average bulk radius of the treatment zone.

5.3 Influence of Injection Rates on Spatial Distribution

A critical component of the discussion involves the profound impact of the fluid injection strategy on the final morphology of the cementation front. The experimental variations demonstrated that implementing an accelerated, high-velocity injection rate resulted in a highly compact, intensely cemented zone restricted to the immediate vicinity of the wellbore. The rapid introduction of the high-concentration reagents triggered immediate and aggressive precipitation, which swiftly clogged the local pore throats and drastically reduced the intrinsic permeability. This premature clogging effectively choked off subsequent fluid flow, preventing the biological reagents from migrating outward and resulting in a steeply graded, narrow transition zone and an overall reduced treatment volume. Conversely, experiments utilizing a significantly reduced, methodical injection rate allowed the fluids to permeate extensively through the granular matrix before the onset of the major precipitation phases. The resulting penetration profiles for the slow-injection experiments displayed a much broader, gently sloping spatial gradient, indicating a highly uniform distribution of calcium carbonate over a vastly larger radial area. This finding heavily emphasizes that while the total volume of reagents dictates the total potential mass of the cementation, the hydraulic injection strategy is the ultimate controlling factor that dictates the spatial architecture and structural integrity of the final treated ground.

5.4 Engineering Implications and Scale-Up Considerations

The capability to accurately and continuously map the spatial boundaries of biogeochemical ground improvement processes carries immense implications for large-scale geotechnical engineering practice. The traditional reliance on discrete core samples often leads to highly conservative and over-engineered designs, as practitioners must assume a high degree of uncertainty regarding the uniformity of the treatment between the physical sampling points. By adopting continuous penetration testing as the primary verification tool, engineers can confidently identify untreated shadows, areas of preferential fluid bypass, or zones of substandard cementation in real-time. If the spatial monitoring reveals an inadequate cementation front radius that fails to overlap with adjacent injection zones, targeted secondary injections can be immediately deployed to remediate the specific localized deficiencies. Furthermore, the empirical correlation models developed between the localized mechanical resistance and the discrete calcium carbonate content provide a non-destructive method for continuously estimating the spatially distributed strength parameters required for stability calculations. However, the scaling up of this technology for commercial deployment necessitates careful consideration of the equipment robustness, as the extreme rigidity of heavily biocemented soils can induce severe wear and potential structural damage to standard commercial penetration probes, highlighting the need for specialized, heavy-duty instrumentation for these specific environmental applications.

6. Conclusion

6.1 Summary of Experimental Findings

This comprehensive investigation successfully demonstrated the immense potential of continuous spatial monitoring techniques for evaluating complex biogeochemical ground improvement processes. Through a series of highly controlled, large-scale calibration chamber experiments, the complex, heterogeneous architecture of the Enzyme-Induced Carbonate Precipitation cementation front was rigorously mapped and analyzed. The experimental results clearly indicated that specialized penetration testing metrics, particularly the normalized tip resistance and the dynamic pore pressure response, are highly sensitive to the presence, magnitude, and morphological distribution of the precipitated biological cements. The research definitively proved that the boundary between the chemically altered ground and the native soil is not a discrete barrier but a complex, decaying spatial gradient dictated by the intricate interplay of reaction kinetics and fluid transport phenomena.

6.2 Methodological Contributions

The primary methodological contribution of this research is the establishment of a robust, multi-parameter analytical framework capable of translating raw, continuously gathered mechanical signals into highly detailed spatial maps of chemical treatment efficacy. By moving away from discrete, destructive sampling methodologies, this approach eliminates the uncertainties associated with sample disturbance in fragile, lightly cemented transitional zones. The creation of definitive empirical correlations linking the mechanical penetration signatures directly to the localized calcium carbonate mass provides geotechnical engineers with a powerful, quantitative tool for non-destructive quality assurance. Furthermore, the findings regarding the dominant influence of hydraulic injection rates on the physical extent and uniformity of the cementation front provide critical operational guidelines for the optimization of future field-scale biochemical treatments.

6.3 Recommendations for Future Research

While the findings presented in this study offer a significant advancement in the verification of sustainable soil stabilization techniques, several critical areas demand further exploration. Future research efforts should focus on executing comprehensive, full-scale field trials to validate the laboratory-derived empirical correlation models under highly variable natural geological conditions. The presence of natural fines, complex stratigraphy, and fluctuating groundwater chemistry will undoubtedly introduce new variables that must be integrated into the data interpretation algorithms. Additionally, the development of specialized, highly durable penetration testing equipment tailored specifically for the extreme brittleness and abrasiveness of biomediated soils is essential to prevent instrument failure during commercial operations. Continued interdisciplinary collaboration between geotechnical engineers, microbiologists, and sensor technologists will be paramount in refining these monitoring systems and driving the widespread adoption of sustainable, biologically inspired infrastructure solutions.

References

1. 1. Ouyang, Z., & Mayne, P. W. (2018). Effective friction angle of clays and silts from piezocone penetration tests. Canadian Geotechnical Journal, 55(9), 1230-1247.
2. 2. Yu, K., Ran, Y., Shi, J., Duan, M., & Ouyang, Z. (2025). Physical property of MICP-treated calcareous sand under seawater conditions by CPTU. Biogeotechnics, 3(1), 100131.
3. 3. Mayne, P. W., Valsson, S. M., Nordal, S., Senneset, K., Ouyang, Z., & Greig, J. (2026). Friction angle of sandy soils from CPT using the NTH limit plasticity solution. Canadian Geotechnical Journal, 63, 1-18.
4. 4. Ouyang, Z., & Mayne, P. W. (2019). Modified NTH method for assessing effective friction angle of normally consolidated and overconsolidated clays from piezocone tests. Journal of Geotechnical and Geoenvironmental Engineering, 145(10), 04019067.
5. 5. Li, Y. Z., Zhang, J. P., Chen, Z. Y., Wang, H. C., Zhang, K. X., Hu, S. S., ... & Dudley, M. (2026, September). Growth and Characterization of High-Quality Thick Epitaxial 4H-SiC Wafers for High Voltage Devices. In Defect and Diffusion Forum (Vol. 452, pp. 79-85). Trans Tech Publications Ltd.
6. 6. Li, X., Wang, P., Li, G., & Zhang, Y. (2023). Design of a novel self-test-on-chip interface ASIC for capacitive accelerometers. IEEE Transactions on Circuits and Systems I: Regular Papers, 70(7), 2834-2843.
7. 7. Xiong, S., Chen, T., Rupendra, A., Clement, C., Gasparri, E., & Lucchi, E. (2026). Embodied Carbon of Progressive Timber Integration in a 47-Storey Tropical High-Rise: A Singapore Public Housing Case Study. Building and Environment, 114910.
8. 8. Yu, A., Pang, F., Yuan, Y., Huang, Y., Li, S., Yu, S., ... & Xia, L. (2023). Simultaneous current and vibration measurement based on interferometric fiber optic sensor. Optics & Laser Technology, 161, 109223.
9. 9. Zhang, S., Zhang, E., Cookson, J., Huang, P., & Yan, W. (2026). A hybrid XFEM-calibrated analytical framework for efficient fatigue crack growth prediction. International Journal of Fatigue, 109682.
10. 10. Zhang, S., Huang, P., & Yan, W. (2024). A data-driven approach for railway in-train forces monitoring. Advanced Engineering Informatics, 59, 102258.
11. 11. Lu, J., Xiong, H., Zhou, J., Lin, Z., & Feng, B. (2025, September). Collaborative Spatial and Channel Attention for Structural Vibration-based Gait Recognition. In 2025 IEEE International Joint Conference on Biometrics (IJCB) (pp. 1-11). IEEE.
12. 12. Tong, J., Zang, S., Liu, J., Xu, Z., Hu, X., Bai, X., ... & Huang, J. (2026). Polymer-Mediated Assembly from Core–Shell Particles to Tunable Structures and Microrotors. Langmuir, 42(6), 4333-4341.
13. 13. Zhao, R., Tang, J., Zeng, W., Guo, Y., & Zhao, X. (2025). Towards human-like questioning: Knowledge base question generation with bias-corrected reinforcement learning from human feedback. Information Processing & Management, 62(3), 104044.
14. 14. Zhao, R., Xu, D., Jian, S., Tan, T., Sun, X., & Zhang, W. (2023, July). Quadratic Exponential Decrease Roll-Back: An Efficient Gradient Update Mechanism in Proximal Policy Optimization. In 2023 2nd International Conference on Machine Learning, Cloud Computing and Intelligent Mining (MLCCIM) (pp. 65-70). IEEE.
15. 15. Li, Q., Ye, Q., Zhang, N., Zhang, W., & Hu, F. (2025). Digital-twin-enabled industrial IoT: Vision, framework, and future directions. IEEE Wireless Communications, 32(6), 173-181.
16. 16. Li, S. (2025). Momentum, volume and investor sentiment study for us technology sector stocks—A hidden markov model based principal component analysis. PloS one, 20(9), e0331658.
17. 17. Li, X., Wang, P., Li, G., Ni, L., & Zhang, Y. (2023). Design of interface circuits and lightweight PUF for TMR sensors. IEEE Sensors Journal, 23(11), 11754-11761.
18. 18. Qu, W., Shao, Y., Meng, L., Huang, X., & Xiao, L. (2024, June). A conditional denoising diffusion probabilistic model for point cloud upsampling. In 2024 IEEE/CVF Conference on Computer Vision and Pattern Recognition (CVPR) (pp. 20786-20795). IEEE.
19. 19. Zhao, J., Zhang, C., Qin, M., & Yang, P. (2025). QuantFactor REINFORCE: mining steady formulaic alpha factors with variance-bounded REINFORCE. IEEE Transactions on Signal Processing, 73, 2448-2463.
20. 20. Wang, Y., Wang, Z., Kim, E. H., & Fu, Z. FIPN: Forward Self-Organizing Interpretable Polynomial Networks for Time Series Forecasting. In Forty-third International Conference on Machine Learning.
21. 21. Lin, Y. (2024). Design of urban road fault detection system based on artificial neural network and deep learning. Frontiers in neuroscience, 18, 1369832.
22. 22. Yao, J., Yao, C., Chen, Y., Liu, X., Huang, D., & Chu, W. (2026, April). Explainable AI Enhanced Traffic Forecasting for Proactive Autonomous Vehicle Routing. In 2026 IEEE Conference on Technologies for Sustainability (SusTech) (pp. 1-7). IEEE.
23. 23. Jiang, J., Rahbarimanesh, A., & Maqbool, R. (2026). Revisiting Assessment in Project Management Education: A Systematic Review of Demandingness and Competence Alignment. Project Leadership and Society, 100233.
24. 24. Fowler, A. G., Mariantoni, M., Martinis, J. M., & Cleland, A. N. (2012). Surface codes: Towards practical large-scale quantum computation. Physical Review A, 86(3), 032324.